Environmental Science Nano

PAPER

View Article Online
View Journal | View Issue

Cite this: *Environ. Sci.: Nano*, 2018, 5, 1640

Closing the gap between small and smaller: towards a framework to analyse nano- and microplastics in aqueous environmental samples†

S. M. Mintenig, *[ab] P. S. Bäuerlein,[b] A. A. Koelmans,[cd] S. C. Dekker[ae] and A. P. van Wezel[ab]

Received 12th February 2018,
Accepted 28th May 2018

DOI: 10.1039/c8en00186c

rsc.li/es-nano

Measuring concentrations and sizes of micro- and nanoplastics in the environment is essential to assess the risks plastic particles could pose. Microplastics have been detected globally in a variety of aquatic ecosystems. The determination of nanoplastics, however, is lagging behind due to higher methodological challenges. Here, we propose a framework that can consistently determine a broad spectrum of plastic particle sizes in aquatic environmental samples. Analytical evidence is provided as proof of principle. FTIR microscopy is applied to detect microplastics. Nanoplastics are studied using field-flow-fractionation and pyrolysis GC-MS that gives information on the particle sizes and polymer types. Pyrolysis GC-MS is shown to be promising for the detection of nanoplastics in environmental samples as a mass of approximately 100 ng is required to identify polystyrene. Pre-concentrating nanoplastics by crossflow ultrafiltration enables polystyrene to be identified when the original concentration in an aqueous sample is >20 μg L^{-1}. Finally, we present an approach to estimate polymer masses based on the two-dimensional microplastic shapes recorded during the analysis with FTIR microscopy. Our suite of techniques demonstrates that analysis of the entire size spectrum of plastic debris is feasible.

Environmental significance

Microplastics have been detected globally in various ecosystems. Recent experimental, modelling and field studies point towards nanoplastics also being present. With a decrease of particle sizes an increase of the particles' toxicity is widely assumed. To assess the risks that are related to plastic litter in the environment, effect and exposure concentrations need to be known and combined. Addressing the latter, we here present a framework that is able to sample and to consistently determine concentrations and sizes of plastics down to a size of 50 nm in an aqueous environmental sample.

1. Introduction

A growing body of literature is documenting the widespread occurrence of plastic litter in various ecosystems[1–3] and its ecological consequences.[4,5] Considerable attention has been given to microplastics (MP): plastics smaller than 5 mm.[6,7] MP and the much smaller particles usually referred to as 'nanoplastics' (NP) can be released into the environment directly[8,9] or can be formed when larger plastic items degrade and fragment under the impact of various environmental stressors.[10–12] The actual fragmentation processes are unknown and currently under research.[13,14] However, it is widely assumed that the fragmentation into small MP and eventually into NP is one of the explanations for the 'missing plastic' budget, a term defined by Cozar *et al.*,[3] who detected lower MP concentrations in the open ocean surfaces than predicted by their model. Recent experimental, modelling and field studies further support this hypothesis.[11–13,15,16]

MP has been studied and detected globally in almost all natural habitats, but no lower size limitations or sub-classes have been officially defined. Yet the term 'nanoplastic' is widely used, but interpreted differently. Here, we primarily acknowledge the formal definition of a nanomaterial by the EU (2011/696/EU),[8,17] according to which at least 50% of the particles must have at least one dimension smaller than 100 nm. Other studies define NP as plastic particles <1 μm[11,16,18] or even <20 μm.[19]

There are currently several protocols for detecting MP,[20] but they lack consistency in sampling, sample pre-treatment,

[a] *Copernicus Institute of Sustainable Development, Utrecht University, The Netherlands. E-mail: s.m.mintenig@uu.nl*
[b] *KWR Watercycle Research Institute, Nieuwegein, The Netherlands*
[c] *Aquatic Ecology and Water Quality Management Group, Wageningen University, The Netherlands*
[d] *Wageningen Marine Research, IJmuiden, The Netherlands*
[e] *Faculty of Management, Science and Technology, Open University, Heerlen, The Netherlands*

† Electronic supplementary information (ESI) available. See DOI: 10.1039/c8en00186c

analysing and reporting of results. The analysis of NP is more elaborate, and protocols are currently under development.[16] One of the major challenges is the pre-concentration of samples required to match the detection limits of currently available instrumentation. The aim of the present paper is twofold. First, we aim to provide a framework for quantitatively analysing NP and MP that is based on three criteria: (a) a sampling strategy to reproducible concentrate plastic particles of targeted sizes, (b) the determination of particle sizes and (c) the identification of polymer types. Second, we aim to provide empirical data on the applicability of novel steps in the proposed framework.

2. A framework for the analysis of nano- and microplastics in aqueous environmental samples

In order to concentrate MP and NP for a representative analysis, starting with an appropriate sampling strategy is of high importance. The protocol used most widely today entails filtering surface water through nets with a mesh size of 333 μm.[1,2,21,22] The size of smaller particles retained is 25 to 45 μm when water is filtered through a stack of sieves,[23,24] and 10 μm when stainless steel cartridge filters are used.[25] Sampling NP is more challenging as conventional filtering is not applicable in these low size ranges. Ter Halle *et al.*[16] used ultrafiltration to concentrate the colloidal fraction (<1.2 μm) of a 1 L seawater sample. Another concentration technique is crossflow ultrafiltration, which uses a filter originally made as dialysis equipment (Hemoflow, Fresenius Medical Care, Germany). This crossflow ultrafiltration setup has been applied successfully to concentrate microorganisms in drinking and surface waters by factors of 4000 and 1000, respectively.[26]

To date, a variety of analytical techniques has been applied to determine MP in environmental samples. Numerous studies have relied on visual sorting of MP of a few hundred μm micrometres in size.[1,27] In recent years, the scientific focus has shifted from determining visible plastic particles to determining microscopic plastic particles, usually using spectroscopic[28–30] or thermal degradation analyses.[31–33] When coupled to a microscope, Fourier transform infrared (FTIR) or Raman spectroscopy reveals the chemical identity of particles and allows the estimation of individual particle sizes and shapes. However, both techniques are limited by particle size: 500 nm for Raman microscopy[29] and 20 μm for FTIR microscopy.[28] In contrast, thermal degradation analyses are not limited by size when analysing mixed environmental samples, but also, they do not provide information on particle sizes. Recent studies have used thermal degradation to identify polymer mixtures in surface water,[16] soil,[31,34] fish[33] and wastewater treatment plant effluents.[32]

A major problem arising from using such different techniques is the incomparability of data.[20,35–37] Manual particle sorting or spectroscopic analyses yield numbers of MP particles or fibres, whereas water volumes,[23,38] surface areas,[2,39] sediment weight[40,41] and suspended particulate matter weight[42] are presented in metric units. A bigger problem occurs when comparing these data with data from thermal degradation procedures that aim to simultaneously identify and quantify polymers[31,33] per sample volume or weight. Eventually, exposure data are needed that can be linked to results generated during effect studies. And as the hazards posed by MP and NP are likely to depend on the concentration, size[5,43] and potentially on polymer types, these data are of high interest.[44,45] Information on polymer masses will be required to enable mass-balance models that link production and emission data to environmental occurrence data.[15,46]

Given that plastic debris comes in a broad spectrum of sizes, its identification requires a combination of different sampling techniques (criterion a) and analytical techniques to determine sizes (criterion b) and polymer types (criterion c) (Fig. 1). The sequence of the techniques, and their relationships, are shown also in a flow scheme (Fig. S1†). In addition to conventional filtration to concentrate MP, we introduce crossflow ultrafiltration to concentrate NMP (nano- and microplastics <20 μm) prior to analysis. For NMP analysis two techniques are needed: asymmetrical flow field-flow fractionation (AF4), which is a versatile tool for sample fractionation based on particle sizes,[47] in combination with pyrolysis gas chromatography-mass spectrometry (GC-MS), to identify polymers in size fractions collected individually. Here, a filtration step is essential since the particle size separation of the AF4 occurs in two modes: in the 'normal' mode, increasing particle sizes lead to an increased retention, whereas this is reversed for bigger particles in the so-called 'steric' mode. The sizes and polymer types of MP particles exceeding 20 μm are identified with micro-FTIR (Fig. 1). Manual sorting and subsequent identification of MP becomes feasible for plastics bigger than 300 μm; thus this common procedure[1,2,20] completes the proposed protocol.

The framework has several components new to this field of research that we have tested individually and in combination. These tests are presented below and comprised (a) sampling surface and drinking water by concentrating them using crossflow ultrafiltration, including the determination of recovery rates, (b) NMP size determination using AF4 and (c) polymer identification of NMP using pyrolysis GC-MS.

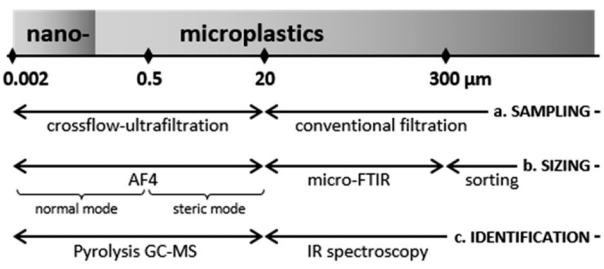

Fig. 1 Protocol applied to: (a) sample; and detect sizes (b) and identify polymer types (c) of nano- and microplastics in an environmental aqueous sample.

3. Materials and methods

3.1 Materials and instrumental setup

Chemicals. Monodispersed NMP suspensions of polystyrene (PS) spheres with specified diameters (50, 100, 200, 500 and 1000 nm) and uncharged surfaces were purchased from Polyscience Inc. (Illinois, USA). Monodispersed gold and silver nanoparticles (50 nm) in solutions with a citrate-based agent were purchased from NanoComposix (California, USA). Green fluorescent MP polyethylene (PE) beads in sizes ranging from 90 to 106 μm were purchased from Cospheric (California, USA). To facilitate dosing, these PE beads were suspended in ultrapure water containing a surfactant (0.01% sodium dodecyl sulphate (SDS), Sigma Aldrich), which yielded a final concentration of 260 mg (5×10^5 particles) L^{-1}. To determine MP number concentrations, the solutions were filtered through cellulose nitrate filters (0.45 μm Whatman, Germany) and PE beads were counted using a dissecting microscope (Zeiss STEMISV8, Germany). Further, transparent PS pellets were cooled with liquid nitrogen, ground and sieved over an installed 100 μm mesh (Retsch Centrifugal Grinding Mill ZM1000, Germany).

Crossflow ultrafiltration. To increase MP and NMP concentrations we used a crossflow ultrafilter (Hemoflow filter HF80S, Fresenius, Medical Care) consisting of bundled hollow fibre membranes made of polysulfone that had an inner diameter of approximately 200 μm. The exact pore sizes were not specified, but the cut-off was defined for proteins sized between 40 and 60 kDa. Samples were pumped (Masterflex, Cole Parmer, USA) through the crossflow ultrafilter at a constant flow rate of 4 L min^{-1} and an overpressure of 0.4 bar. Thereby the permeate was pressed through the filter while the concentrate was retained and rinsed back into the tank, raising particle concentrations (see Fig. S2†).

AF4. An AF4 system was used (Postnova Analytics GmbH, AF2000, Landsberg, Germany), coupled online to a UV detector (Shimadzu) and a multi-angle light-scattering (MALS) detector (Postnova, Landsberg, Germany). The trapezoidal channel was 27.5 cm long and 250 μm thick. There were two membranes, 10 kDa regenerated cellulose (RC) and 10 kDa polyethersulfone (PES) (Postnova, Landsberg, Germany), and three carrier liquids: ultrapure water (>18 MΩ), a solution containing an anionic surfactant (0.01% SDS, Sigma Aldrich) and a solution containing a non-ionic surfactant (0.01% TWEEN, Sigma Aldrich) surfactant (see Table S1†). The fractionation and presence of particles were recorded by the MALS detector. Plotting the detection signal against the fractionation time, the area under the curve (AUC), proportional to the particle concentrations injected, was determined using GraphPad Prism (5.01, GraphPad Software, San Diego California USA). Further information on the general ability and limitations of the AF4 to separate particles can be found elsewhere.[48,49]

Pyrolysis GC-MS. Polymers in environmental samples were analysed using pyrolysis GC-MS. The samples were pyrolysed at 560 °C (Pyromat, GSG Mess- und Analysegeräte, Germany) in a tubular pyrolysis wire with a capacity of approximately 15 μL. The instrumental details for pyrolysing a sample are provided as ESI† (Table S2). The degradation gases were separated using a GC (Trace GC, ThermoFisher Scientific, Madison, USA) and identified using an MS system (Trace MS Plus, ThermoFisher Scientific, Madison, USA). The settings of the GC-MS system are shown in Table S3.† Generated pyrograms, peak intensities and polymer characteristic mass-to-charge (m/z) ratios were analysed using the software XCalibur (Thermo XCalibur 2.2 SP1.48, ThermoFisher Scientific, Madison, USA). Individual compounds were searched within a library of organic compounds (NIST/EPA/NIH MS Library (NIST 11), USA) and an in-house generated library.

Micro-FTIR. An FTIR microscope equipped with an ultrafast motorized stage and a single mercury cadmium telluride (MCT) detector (Nicolet iN10, ThermoFisher Scientific, Madison, USA) was used to identify MP, using chemical mapping. This entailed enrichment of the samples on aluminium oxide filters (Anodisc 25 mm, Whatman, UK) placed on a calcium fluoride (CaF_2) crystal (EdmundOptics, Germany) to prevent filter bending. All measurements were taken in transmission mode (Löder *et al.*[28]). Polymers were identified with the aid of the "Hummel Polymer and Additives FTIR Spectral Library" (ThermoFisher Scientific, Madison, USA). The spectra and chemical maps generated were analysed using Picta software (1.5.120, ThermoFisher Scientific, Madison, USA).

Samples. To test the individual techniques that make up the framework, samples of drinking and surface water were spiked with different monodispersed plastic particles. The drinking water was tapwater from Nieuwegein; the ultrapure water was obtained by purifying demineralized water in a Milli-Q system (Millipore, MA, USA). The surface water samples were from two freshwater systems in the Netherlands: the Lek canal and Lake IJssel. The Lek canal was sampled in April 2016 using a stainless steel bucket. Surface water of Lake IJssel was sampled using crossflow ultrafiltration (Fig. S2†) in January 2016. Using a water standpipe at an official sampling point, we obtained surface water pumped from a depth of 0.5 m by placing a small stainless steel cask with a volume of approximately 20 L under the open tap and allowing it to fill with water. The volume of water was maintained at a constant level by means of a float valve that allowed more water to be pumped into the cask automatically when the level fell. This allowed the concentration process to proceed unsupervised for 24 h. During this time, 635 L surface water were filtered and concentrated into a volume of 0.4 L. Contamination with plastic particles was minimized by using tubes rinsed with ultrapure water and by covering the tank with aluminium foil. Subsequently, the Lake IJssel sample was filtered through a 20 μm stainless steel sieve, the retentate was treated with 1 M sodium hydroxide (NaOH, 3 days, 50 °C, similar to Dehaut *et al.*[50]). During sample handling cotton lab coats were worn at all times and the sample was kept covered whenever possible. Further controls and blanks could be omitted because spiked particles were used.

3.2 Testing the analytical framework using spiked environmental samples

A) Sampling. Crossflow ultrafiltration was further validated by adding NMP (PS 50 and 200 nm) or MP (PE 90-120 μm) to drinking water samples. The drinking water came directly from the tap and was not filtered before usage. For both plastic types, three 100 L samples were concentrated into final volumes of 0.5 L. Further, one sample of pure drinking water was filtered and used as a blank. For MP, the starting concentration was 2.6 μg (5 particles) L^{-1}. For NMP, 0.4 mg L^{-1} PS (50 nm) and 0.585 mg L^{-1} (200 nm) PS were added. Standard suspensions with particle concentrations 200 times higher than indicated concentrations were produced and used to determine NMP recovery rates. Preconcentration was done as follows: the 100 L samples were distributed among five jerry cans (20 L, HDPE) and pumped through the crossflow ultrafilter. Each jerry can was thoroughly rinsed with ultrapure water and ethanol (30%). After two hours the concentrate was collected in a glass jar, and the tubes and filters were rinsed twice by pumping 150 mL of collected permeate through the filter. The MP beads were counted using a dissecting microscope and the numbers compared to the originally admixed concentrations. The NMP samples and standard suspension were analysed in quadruplicate using AF4-MALS, and the AUCs were determined. Because this AUC is proportional to a NMP concentration range of 0.1 to 140 mg L^{-1} ($R^2 > 0.99$), it was used to evaluate the NMP recovery. In addition to AF4-MALS measurements, all NMP samples were re-analysed using spectrophotometry (UNICAM UV 500, ThermoSpectronic). The UV absorbance was measured at 229 nm wavelength, at which PS in ultrapure water shows the highest absorption. The system was calibrated for PS concentrations between 4 to 23.6 mg L^{-1}, resulting in a linear increase of measured absorbance ($R^2 > 0.99$). The UV absorbance of the concentrated crossflow samples was measured after samples had been diluted with ultrapure water (1 : 10) and ultrasonicated for five minutes to prevent erroneous measurements arising from aggregation.

B) Size determination. To detect the sizes of plastics accurately, different techniques were used. For MP, the two-dimensional shape (maximum and minimum diameters) of individual particles can be assessed during chemical mapping by using micro-FTIR, as will be explained in the following section. More challenging is the size determination for NMP; although AF4 is a powerful technique for separating a variety of nanoparticles, it needs to be adapted for the particles of interest.[47] First, two membranes, RC and PES, were tested in combination with different carrier liquids: ultrapure water, or a solution containing an anionic (SDS) or a non-ionic (TWEEN) surfactant. These surfactants were added to reduce particle–membrane interactions that could cause erroneous results. Each combination was evaluated using the data recorded by the MALS detector. We tested for distinct signals by injecting monodispersed NMP suspension (50 and 500 nm, 50 mg L^{-1}, injection volume of 30 μL). To test for complete size separation we injected a mixture of 50, 100, 200, and 500 nm spheres (each 200 mg L^{-1}, 20 μL). The settings to run the AF4 system are presented in Table S1;† using these, the elution times of the various NMP sizes were recorded. In a second step, a monodispersed suspension of 1000 nm spheres (200 mg L^{-1}, 10 μL) was injected to determine elution time and signal intensity recorded by the MALS detector. A new mixture of all five NMP sizes was analysed under different crossflow conditions (0.5, 1, 2, 3, 4 mL min^{-1}, Table S1†) to test if a simultaneous separation might be feasible or if there had been a transition from the "normal mode" to the "steric mode". This was done because previous studies have shown that this transition occurs for particle sizes of about 1 μm.[47,51] The MALS detector provides data on the particles' radii. For a concentration range for particles of 50 and 200 nm (100–0.1 mg L^{-1}, 50 μL) it was determined when discernible peaks were detected compared to the baseline and when the particle sizes given by the MALS detector matched the supplier's specifications.

NMPs are made of polymers with different densities. To test the effect of different densities on the elution times of particles, we injected monodispersions of 50 nm PS, gold and silver nanoparticles.

C) Polymer identification. The final polymer characterization was also conducted using two techniques, pyrolysis GC-MS for NMPs and micro-FTIR for MP. Pyrolysis GC-MS was used to determine the presence of polymers in size fractions previously separated by AF4. Lek canal and Lake IJssel surface waters were examined using pyrolysis GC-MS. To do so, pyrolysis tubes were filled with 12.5 μL sampled water, and the water evaporated at 60 °C. This step was repeated resulting in a total sample volume of 25 μL. The sample from the Lek canal was tested solely for PS (200 nm) that had been added at concentrations of 0.6 mg L^{-1} (mimicking the status before crossflow ultrafiltration), 117 mg L^{-1} (after crossflow ultrafiltration) and 1200 mg L^{-1}, resulting in PS masses of 15 ng, 3 μg and 30 μg within the sample volumes of 25 μl. These tubes were pyrolysed several times (Table S2†) to ascertain whether full material pyrolysis occurred and, if so, when. The analysis focussed on characteristic PS degradation products: styrene (mass 104) and tristyrene (mass 312).[33] Fischer and Scholz-Böttcher[33] showed that the more abundant styrene is non-specific, since it is also produced when chitin is pyrolysed. In contrast, the tristyrene is less abundant, but specific for the presence of PS.

Finally, PS was added to the organic rich Lake Ijssel sample in PS concentrations of 1 to 20 mg L^{-1}. Pyrolysis tubes were filled with 25 μl of these solutions, and thus contained 25 to 500 ng PS. The limit of detection (LOD) was determined based on an S/N ratio of 3; the limit of quantification (LOQ) was assessed considering an S/N ratio of 10.

The second technique used was micro-FTIR to identify MP. In order to measure MP down to 20 μm in a feasible time frame, when using micro-FTIR equipped with a single MCT detector, we tested filter surface chemical mapping at

two spectral and spatial resolutions. For all measurements, the aperture size was set at 50 × 50 μm. The spatial resolution, *i.e.* the step sizes between measurement points, was set at 20 or 35 μm. In combination with the changed step sizes, we tested a spectral resolution of 8 cm^{-1} with four scans per point and of 16 cm^{-1} with one scan per point (ultra-fast mapping option). To do so, PS fragments (9 to 90 μm) were spread on an Anodisc filter. The area of the mapped filter area covered with PS as well as the particle numbers were determined using Picta software.

4. Results

4.1 NMP recovery using crossflow ultrafiltration

The recovery rates of NMP and MP particles were evaluated after concentrating drinking water samples by crossflow ultrafiltration. The three samples revealed an MP recovery of 50.2% (±11.9). The NMP samples were analysed using AF4-MALS and spectrophotometry and both methods yielded a reproducible NMP recovery (Fig. 2, Table 1). Spectrophotometry yielded a total NMP (50 and 200 nm PS) recovery of 54.0% (±2, n = 3). During AF4 separation the MALS detector revealed that the peak of the 200 nm spheres was less intense, broader and lagged behind after crossflow concentration. The 50 nm NP hardly peaked (Fig. 2). The recovery rates calculated using the AUCs were 49.3% (±3.7, n = 3) for the 200 nm particles and 12.7% (±1.3, n = 3) for the 50 nm spheres, which together makes a total NMP recovery of 48.6% (±3.6, n = 3) (Table 1). The values are within the error ranges of the measurements of the total recovery determined earlier. Further, the MALS detector specified average radii of 115 nm (±1.5, n = 125) and 53 nm (±2.4, n = 28) for the concentrated samples and of 111 nm (±0.5, n = 73) and 67 nm (±1.9, n = 19) for the standard suspension analysed (Fig. 2). The variations might be attributable to matrix effects yet suggest that homo-aggregation during the concentration was not relevant.

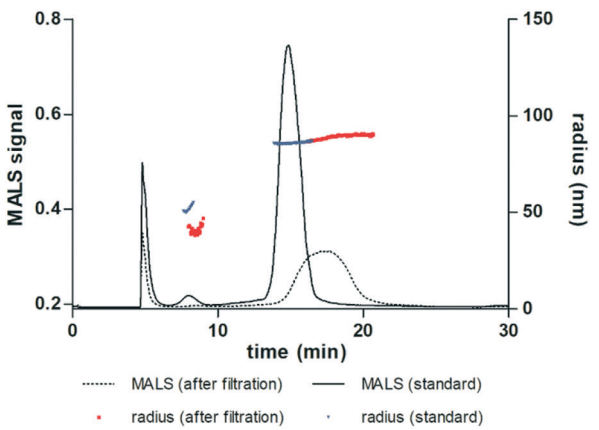

Fig. 2 MALS signal and NMP radii in drinking water after crossflow ultrafiltration and in the standard suspension containing calculated target concentrations.

Table 1 Recovery of NMP (measured with AF4-MALS[a] and UV-vis spectrophotometry[b]) and MP[c] after concentrating 100 L of drinking water with crossflow ultrafiltration

	Initially added plastics	Recovery (%)	SD
NMP	50 nm (0.4 mg L^{-1})[a]	12.7	1.3
	200 nm (0.585 mg L^{-1})[a]	49.3	3.7
	50 + 200 nm[a]	48.6	3.6
	50 + 200 nm[b]	54.0	2.0
MP	(2.6 μg L^{-1})[c]	50.2	11.9

4.2 Size determination of NMP using asymmetrical flow field-flow fractionation (AF4)

First, two membranes, RC and PES, were tested in combination with different carrier liquids. As only the RC membrane and the 0.01% SDS solution led to distinct peaks and a satisfactory size separation (Table S4†), this combination was chosen for further tests. A complete size separation of PS spheres in a polydispersion (50, 100, 200 and 500 nm) was possible. Although the 200 and 500 nm peaks were close, they were still distinguishable (Fig. 3A).

In a second step, a monodisperse suspension of 1000 nm spheres (200 mg L^{-1}, 10 μL) was injected. These particles had a similar elution time as the 200 and 500 nm spheres under crossflow conditions of 2 mL min^{-1} (Fig. 3B). A new mixture of these five NMP sizes was analysed under different crossflow conditions (0.5, 1, 2, 3, 4 mL min^{-1}, Table S1†) but none of these could fractionate particles of 1000 nm successfully,

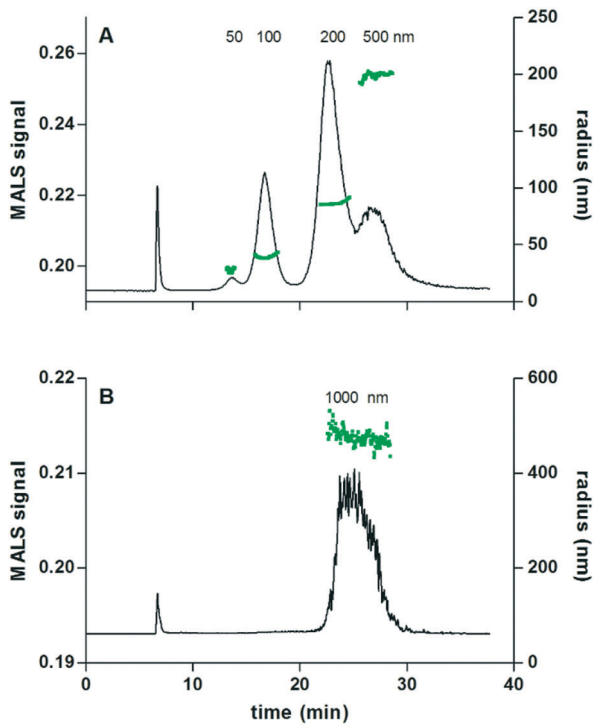

Fig. 3 MALS signal (black line) and NMP radii (green dots) when analysing (A) a polydispersion of 50, 100, 200 and 500 nm spheres and (B) a monodispersion of 1000 nm spheres.

which implies that transition from the "normal mode" to the "steric mode" occurred, and that prior to analysis, particles larger than 500 nm need to be removed by filtration. The scope of the present study did not allow a further, detailed evaluation of particle fractionation in the steric mode.

The MALS detector indicated average particle sizes of 72 nm (±4.3, n = 23), 103 nm (±3.8, n = 60), 225 nm (±4.5, n = 76) and 514 nm (±7.1, n = 85) (Fig. 3A), and further 1233 nm (±41.7, n = 161) (Fig. 3B), which fairly matches the characteristics of originally injected spheres. For particles of 50 and 200 nm (100–0.1 mg L^{-1}, 50 μL) the concentration range was determined where distinguishable peaks were detected and where particle sizes were in accordance with the supplier's specifications. The particles of 200 nm were still detected correctly at a PS concentration of 1 mg L^{-1}, but not at a concentration of 0.5 mg L^{-1}. For particles of 50 nm the detection limit was between 5 and 10 mg L^{-1}. In combination with preconcentration using crossflow ultrafiltration, these LODs would further decrease by 200 times, resulting in values between 5 and 50 μg L^{-1}.

Lastly, to test the effect of different particle densities on the elution times of particles, monodispersions of 50 nm PS, gold and silver nanoparticles were injected. Using the same settings, the particles eluted at the same time (Fig. 4), indicating that different polymer densities will not hinder a satisfactory size fractionation of NMP.

4.3 Identification of NMP using pyrolysis GC-MS

First, samples from the Lek canal with added PS masses of 15 ng, 3 μg and 30 μg were analysed and examined for the presence of the styrene (mass 104) and tristyrene (mass 312) (Fig. S3†). Compared with the values detected for 3 μg PS, the styrene intensity for 30 μg PS was ten times higher but the tristyrene intensity was only twice as high, indicating that pyrolysis of the material was incomplete. Although this does not hamper polymer identification, it might hamper a quantification with one run.

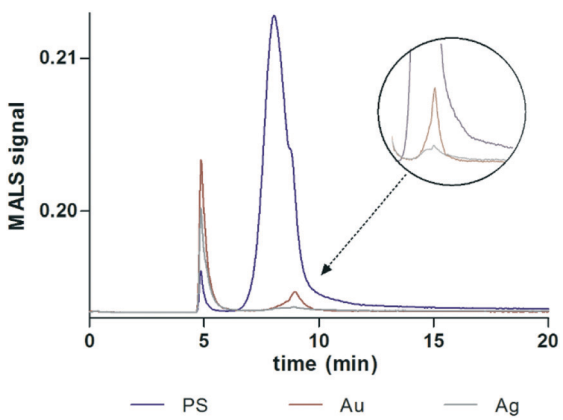

Fig. 4 MALS signal revealed similar elution times for nanoparticles (50 nm) made of PS, gold and silver.

Secondly, pyrolysis tubes containing masses of 25 to 500 ng PS in organic-rich surface water were analysed to ascertain the LOD and LOQ of this method. The styrene was detected in all pyrolysis tubes with lower PS concentrations (Fig. S3†). The tristyrene was identified for PS of at least 100 ng (S/N ratio of 7). As tristyrene is specific for PS, the analysis should focus on this compound, which will result in an LOD between 50 and 100 ng and an LOQ between 100 and 250 ng for environmental samples. Under the given settings and pyrolysed volumes of 25 μL, an LOD of 4 mg L^{-1} and an LOQ of 4–10 mg L^{-1} were assessed.

4.4 Identification of MP using micro-FTIR

Using different spectral and spatial resolutions during chemical mapping yielded slightly varying PS-covered areas and particle counts between the step sizes of 20 μm (29 particles and 9.4%; 32 particles and 9.2%) and 35 μm (25 particles and 9.3%; 28 particles and 10.6%). Step sizes of 20 μm were preferred since we aimed to detect small MP for which information would be lost if step sizes were bigger. Further, the smaller step sizes allow a more precise determination of sizes and numbers for particles that lie close to each other. Both spectral resolutions yielded spectra of sufficient quality to identify polymer types. We used the lower spectral resolution for further measurements, since it required shorter measuring times.

Based on data generated during micro-FTIR analysis we estimated polymer masses using the length (l), width (w) and depth (d) of the particles and their density. While the two-dimensional shape of each particle ($l \times w$) can be assessed from the micro-FTIR data, the third dimension (d) cannot be measured. However, we can assume that the particles will prefer a 'flat' position on the filter, implying that the unknown third dimension (d) will be the smallest of the three. Consequently, it can be assumed that particles on average have a third dimension which is half of the second dimension. This assumption will become accurate when the number of particles is sufficiently large.

4.5 Evaluation of the proposed framework

Several techniques are needed in order to determine a wide size range of plastics. The framework we present makes it possible to concentrate NMP and MP, and to identify and quantify the sizes and polymer types of various NMPs and MPs in an aqueous environmental matrix. During this study, individual techniques were tested that proved to be promising for application in this field of research (Fig. 5). The approach is in parts comparable to the one presented recently by Ter Halle *et al.*[16] who sampled plastic of various sizes in the North Atlantic. They applied micro-FTIR for MP detection >25 μm and a combination of dynamic light scattering (DLS) and pyrolysis GC-MS to identify plastics <1.2 μm.

Compared to the techniques' theoretical size constraints as presented in Fig. 1, only slight adaptions needed to be made (Fig. 5). Using a micro-FTIR that is not equipped with

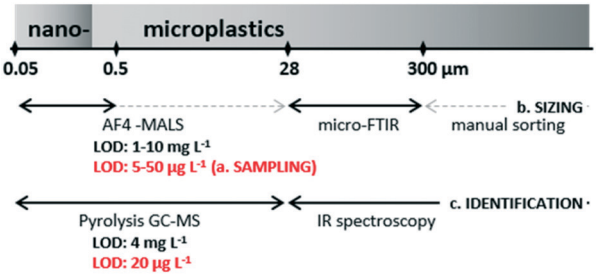

Fig. 5 Overview of techniques applied, showing respective size and concentration limitations. Using a crossflow filter, particles were concentrated by a factor of 200, which further decreased the LODs.

an advanced focal plane array detector which can measure several pixels at the same time[28,51] we suggest mapping the surface of a filter in steps of 20 μm at a reduced spectral resolution. This enables MP down to 28 μm to be determined. To assess polymer masses from the generated results, we propose a particle shape analysis. Although based on an assumption about the particles' third dimension, this approach offers a solution for combining MP and NMP data not only within the framework presented, but also in studies in general.

NMP particles are examined using a combination of AF4-MALS and pyrolysis GC-MS. The AF4-MALS was tested and the settings optimized to allow NMP between 50 and 500 nm to be separated. Based on these settings and depending on the particle sizes, the coupled MALS detector detected particle sizes for PS concentrations of 1–10 mg L^{-1}. In our approach, the AF4-MALS sample fractionation is based on previously determined elution times and thus, is not concentration-dependent. Subsequently, individual fractions are analysed using pyrolysis GC-MS. Although there is no size limitation, a minimum of approximately 100 ng is required to guarantee the detection of PS in an environmental matrix. Based on the analysed sample volume of 25 μL, a concentration of 4 mg L^{-1} PS would be required.

To decrease the LODs, particles need to be concentrated during sampling. To do so, we introduced crossflow ultrafiltration and determined that NMP were recovered reproducibly for sample volumes of 100 L. At a concentration factor of 200, the LOD for originally present particles would decrease to 20 μg L^{-1}. Recommendations for addressing the remaining "gaps" in the NMP–MP size continuum (dashed lines, Fig. 5) of the proposed framework are discussed below.

5. Discussion

5.1 Closing the gap between small and smaller

The field of micro- and nanoplastic research is relatively young, implying that methods are still under development. So far, the use of FTIR or Raman microscopy has been favoured for the examination of MP at micrometre sizes. Although these techniques enable sizes, shapes and polymer types to be detected simultaneously, they have shortcomings regarding detectable particle sizes, their semi-quantification and their long measurement and data analysis times. As previous studies[16,28] have noted, it is preferable to analyse whole samples, especially if they are very heterogeneous. However, this is laborious and time-consuming. Of great benefit is an automatic approach to handle data generated by micro-FTIR, reducing the workload and increasing objectivity and comparability of the data generated.[52] In addition, the particle shape analysis we propose enables the relationship between data derived from spectroscopic and thermal degradation methods to be ascertained. Recently, polymer mixtures in environmental matrices have been determined using thermogravimetric analysis (TGA),[31] or pyrolysis[16,33] coupled to a GC-MS system. A TGA system offers controlled continuous heating with a simultaneous weight loss determination and sample volumes of 20 mg soil.[31] Using pyrolysis GC-MS and sample volumes of 1 mg, Fischer and Scholz-Böttcher[33] evaluated the LOD and LOQ for various polymer types in fish samples and were constrained only by the scale used (repeatability of 0.25 μg). They therefore expect these limits to lie in the range of nanograms, which makes thermal degradation methods appealing for detecting NMP.

As already mentioned, micro- and nanoplastic sizes should be routinely provided, due to size-related effects[45] and to enable comparisons with other studies. Using AF4 and analysing individual size fractions generates broad and valuable results.

This could complement the protocol proposed by Ter Halle *et al.*[16] using DLS and pyrolysis GC-MS. In comparison with DLS, the size determination using AF4-MALS is not concentration-dependent but is based on *a priori* determined elution times of injected NMP standards (Fig. 3A). Applying DLS for heterogeneous samples might cause misinterpretation of particle sizes and an underestimation of very small particles.[47] The different polymer densities will not hinder a satisfactory separation, as separation is dependent on particle sizes, not densities. We did not elaborate on the particle fractionation in the steric mode, but after Dou *et al.*[53] separated PS spheres from 1 μm up to 40 μm satisfactorily, we conclude the AF4 being appropriate to fill the remaining gap in the proposed protocol (Fig. 5).

5.2 Sampling and sample preparation

Adequate sampling of NMP to reach methodological detection limits of further analyses is especially challenging. We propose using crossflow ultrafiltration to concentrate NMP. To evaluate this technique, we tested NMP recovery and potential aggregation processes. Although reproducible, the recovery of the 50 nm spheres was not yet at its full potential (Table 1). The crossflow ultrafilters are used as dialysis equipment and are made to retain proteins of 60 kDa. SEM microscopy might be used to test if damaged membranes were limiting the recovery of 50 nm spheres, or if the current limitation could be attributed to attachments on the inner walls of the equipment used. Doses of a surfactant in low concentrations might reduce particle–membrane and

attachment interactions and subsequently increase the recovery rates. Further, we demonstrate the potential of the this crossflow ultrafiltration setup for sampling surface waters: 635 L were filtered and the particles concentrated into a volume of 0.4 L, which corresponds to a concentration factor of 1580. This might be increased by a subsequent ultrafiltration.[16] Ter Halle *et al.*[16] concentrated surface water samples of 1 L using ultrafiltration in a polysulfone-based cell. The filtration had to be repeated several times because the cell volume was 180 ml, but they succeeded in reducing the sample volume to 10 ml – a concentration factor of 200.

Although we tested the fibrous crossflow ultrafiltration membranes with an inner diameter of approximately 200 μm for filtering MP of 100 μm size, we suggest to combine conventional filtration, *e.g.* with stacked sieves, with crossflow ultrafiltration (Fig. S1†). Using sieves of *e.g.* 20 μm, 300 μm and 1 mm allows for large volumes of water to be filtered, as larger particles would no longer clog the membrane used during crossflow ultrafiltration.

A further point to consider is sample preparation. This is already laborious for MP, but will be even more challenging for NMP. Several approaches have been presented for MP, but studies are now focusing on an enzymatic[25,33,54–56] or alkaline[50,57,58] treatment to reduce the organic sample matrix while inorganic particles are removed conducting a density separation. As our study aim was to test the handling and applicability of individual techniques, we did not include contamination controls. Though often neglected, these tests are needed when analysing environmental samples to determine a method's representability and reliability. Positive controls need to assess if and how much NMP adsorbs to filter or filter equipment when filtering NMP prior to AF4 analysis. The negative controls are particularly important given the broad usage of plastic materials and the frequently discussed contamination with synthetic fibres.[20,59]

Conclusion and outlook

The presented analytical framework contributes to a more consistent determination of a broad size spectrum of plastic particles, including nanoplastics, in aqueous environmental samples. We have shown empirical data on the applicability of the techniques used to sample, to determine plastic sizes and to identify polymer types. The sampling is especially challenging for NMP, but crossflow ultrafiltration proved to reproducibly concentrate these. By doing so, it completes conventional filtration methods.

The data this framework generates will help elucidate environmental fate (including fragmentation processes), will allow a system-based mass balance to be achieved and, ultimately, will allow assessing environmental risks of micro- and nanoplastics.

Conflicts of interest

There are no conflicts to declare.

Acknowledgements

This study was funded by the Dutch Technology Foundation TTW (project number 13940). We acknowledge additional support from and discussions with representatives from KWR, IMARES, NVWA, RIKILT, the Dutch Ministry of Infrastructure and the Environment, The Dutch Ministry of Health, Welfare and Sport, Wageningen Food & Biobased Research, STOWA, RIWA and the Dutch water boards (BTO Joint Research Program). Thanks to J. Burrough for advising on the English.

References

1 T. Mani, A. Hauk, U. Walter and P. Burkhardt-Holm, Microplastics profile along the Rhine River, *Sci. Rep.*, 2015, **5**, 1–7.
2 K. L. Law, S. E. Moret-Ferguson, D. S. Goodwin, E. R. Zettler, E. De Force, T. Kukulka and G. Proskurowski, Distribution of Surface Plastic Debris in the Eastern Pacific Ocean from an 11-Year Data Set, *Environ. Sci. Technol.*, 2014, **48**, 4732–4738.
3 A. Cozar, F. Echevarria, J. I. Gonzalez-Gordillo, X. Irigoien, B. Ubeda, S. Hernandez-Leon, A. T. Palma, S. Navarro, J. Garcia-de-Lomas, A. Ruiz, M. L. Fernandez-de-Puelles and C. M. Duarte, Plastic debris in the open ocean, *Proc. Natl. Acad. Sci. U. S. A.*, 2014, **111**, 10239–10244.
4 S. Kühn, E. L. Bravo Rebolledo and J. A. Van Franeker, in *Marine Anthropogenic Litter*, ed. M. Bergmann, L. Gutow and M. Klages, Springer, Berlin, 2015, ch. 4, pp. 75–116.
5 C. B. Jeong, E. J. Won, H. M. Kang, M. C. Lee, D. S. Hwang, U. K. Hwang, B. Zhou, S. Souissi, S. J. Lee and J. S. Lee, Microplastic Size-Dependent Toxicity, Oxidative Stress Induction, and p-JNK and p-p38 Activation in the Monogonont Rotifer (Brachionus koreanus), *Environ. Sci. Technol.*, 2016, **50**, 8849–8857.
6 C. Arthur, J. Baker and H. Bamford, in *Proceedings of the International Research Workshop on the Occurence, Effects and Fate of Microplastic Marine Debris*, 9-11 September 2008, NOAA Technical, Memorandum NOS-OR&R30, 2009.
7 A. J. Verschoor, *Towards a definition of microplastics - Considerations for the specification of physico-chemical properties*, National Institute for Public Health and the Environment, Bilthoven, The Netherlands, 2015.
8 A. A. Koelmans, E. Besseling and W. J. Shim, in *Marine Anthropogenic Litter*, ed. M. Bergmann, L. Gutow and M. Klages, Springer International Publishing, Cham, 2015, pp. 325–340, DOI: 10.1007/978-3-319-16510-3_12.
9 L. M. Hernandez, N. Yousefi and N. Tufenkji, Are There Nanoplastics in Your Personal Care Products?, *Environ. Sci. Technol. Lett.*, 2017, **4**, 280–285.
10 B. Gewert, M. M. Plassmann and M. MacLeod, Pathways for degradation of plastic polymers floating in the marine environment, *Environ. Sci.: Processes Impacts*, 2015, **17**, 1513–1521.
11 S. Lambert and M. Wagner, Characterisation of nanoplastics during the degradation of polystyrene, *Chemosphere*, 2016, **145**, 265–268.

12 J. Gigault, B. Pedrono, B. Maxit and A. Ter Halle, Marine plastic litter: the unanalyzed nano-fraction, *Environ. Sci.: Nano*, 2016, **3**, 346–350.
13 Y. K. Song, S. H. Hong, M. Jang, G. M. Han, S. W. Jung and W. J. Shim, Combined Effects of UV Exposure Duration and Mechanical Abrasion on Microplastic Fragmentation by Polymer Type, *Environ. Sci. Technol.*, 2017, **51**, 4368–4376.
14 J. E. Weinstein, B. K. Crocker and A. D. Gray, From macroplastic to microplastic: Degradation of high-density polyethylene, polypropylene, and polystyrene in a salt marsh habitat, *Environ. Toxicol. Chem.*, 2016, **35**, 1632–1640.
15 A. A. Koelmans, M. Kooi, K. L. Law and E. V. Sebille, All is not lost: Deriving a top-down mass budget of plastic at sea, *Environ. Res. Lett.*, 2017, **12**, 114028.
16 A. Ter Halle, L. Jeanneau, M. Martignac, E. Jardé, B. Pedrono, L. Brach and J. Gigault, Nanoplastic in the North Atlantic Subtropical Gyre, *Environ. Sci. Technol.*, 2017, **51**, 13689–13697.
17 K. Mattsson, L. A. Hansson and T. Cedervall, Nano-plastics in the aquatic environment, *Environ. Sci.: Processes Impacts*, 2015, **17**, 1712–1721.
18 J. P. da Costa, P. S. M. Santos, A. C. Duarte and T. Rocha-Santos, (Nano)plastics in the environment – Sources, fates and effects, *Sci. Total Environ.*, 2016, **566**, 15–26.
19 M. Wagner, C. Scherer, D. Alvarez-Muñoz, N. Brennholt, X. Bourrain, S. Buchinger, E. Fries, C. Grosbois, J. Klasmeier, T. Marti, S. Rodriguez-Mozaz, R. Urbatzka, A. D. Vethaak, M. Winther-Nielsen and G. Reifferscheid, Microplastics in freshwater ecosystems: what we know and what we need to know, *Environ. Sci. Eur.*, 2014, **26**, 1–9.
20 M. Filella, Questions of size and numbers in environmental research on microplastics: methodological and conceptual aspects, *Environ. Chem.*, 2015, **12**, 527–538.
21 M. Eriksen, S. Mason, S. Wilson, C. Box, A. Zellers, W. Edwards, H. Farley and S. Amato, Microplastic pollution in the surface waters of the Laurentian Great Lakes, *Mar. Pollut. Bull.*, 2013, **77**, 177–182.
22 V. Hidalgo-Ruz, L. Gutow, R. C. Thompson and M. Thiel, Microplastics in the Marine Environment: A Review of the Methods Used for Identification and Quantification, *Environ. Sci. Technol.*, 2012, **46**, 3060–3075.
23 S. A. Carr, J. Liu and A. G. Tesoro, Transport and Fate of Microplastic Particles in Wastewater Treatment Plants, *Water Res.*, 2016, **91**, 174–182.
24 S. Ziajahromi, P. A. Neale, L. Rintoul and F. D. L. Leusch, Wastewater treatment plants as a pathway for microplastics: Development of a new approach to sample wastewater-based microplastics, *Water Res.*, 2017, **112**, 93–99.
25 S. M. Mintenig, I. Int-Veen, M. G. J. Löder, S. Primpke and G. Gerdts, Identification of microplastic in effluents of waste water treatment plants using focal plane array-based micro-Fourier-transform infrared imaging, *Water Res.*, 2017, **108**, 365–372.
26 H. R. Veenendaal and A. J. Brouwer-Hanzens, *A method for the concentration of microbes in large volumes of water*, 2007.
27 M.-T. Nuelle, J. H. Dekiff, D. Remy and E. Fries, A new analytical approach for monitoring microplastics in marine sediments, *Environ. Pollut.*, 2014, **184**, 161–169.
28 M. G. J. Löder, M. Kuczera, S. Mintenig, C. Lorenz and G. Gerdts, Focal plane array detector-based micro-Fourier-transform infrared imaging for the analysis of microplastics in environmental samples, *Environ. Chem.*, 2015, **12**, 563–581.
29 A. Käppler, F. Windrich, M. G. J. Loder, M. Malanin, D. Fischer, M. Labrenz, K. J. Eichhorn and B. Voit, Identification of microplastics by FTIR and Raman microscopy: a novel silicon filter substrate opens the important spectral range below 1300 cm(-1) for FTIR transmission measurements, *Anal. Bioanal. Chem.*, 2015, **407**, 6791–6801.
30 H. K. Imhof, C. Laforsch, A. C. Wiesheu, J. Schmid, P. M. Anger, R. Niessner and N. P. Ivleva, Pigments and plastic in limnetic ecosystems: A qualitative and quantitative study on microparticles of different size classes, *Water Res.*, 2016, **98**, 64–74.
31 E. Dümichen, P. Eisentraut, C. G. Bannick, A.-K. Barthel, R. Senz and U. Braun, Fast identification of microplastics in complex environmental samples by a thermal degradation method, *Chemosphere*, 2017, **174**, 572–584.
32 M. Majewsky, H. Bitter, E. Eiche and H. Horn, Determination of microplastic polyethylene (PE) and polypropylene (PP) in environmental samples using thermal analysis (TGA-DSC), *Sci. Total Environ.*, 2016, **568**, 507–511.
33 M. Fischer and B. M. Scholz-Böttcher, Simultaneous Trace Identification and Quantification of Common Types of Microplastics in Environmental Samples by Pyrolysis-Gas Chromatography–Mass Spectrometry, *Environ. Sci. Technol.*, 2017, **51**, 5052–5060.
34 E. Dümichen, A.-K. Barthel, U. Braun, C. G. Bannick, K. Brand, M. Jekel and R. Senz, Analysis of polyethylene microplastics in environmental samples, using a thermal decomposition method, *Water Res.*, 2015, **85**, 451–457.
35 S. M. E. Cannon, J. L. Lavers and B. Figueiredo, Plastic ingestion by fish in the Southern Hemisphere: A baseline study and review of methods, *Mar. Pollut. Bull.*, 2016, **107**, 286–291.
36 Y. K. Song, S. H. Hong, M. Jang, G. M. Han, M. Rani, J. Lee and W. J. Shim, A comparison of microscopic and spectroscopic identification methods for analysis of microplastics in environmental samples, *Mar. Pollut. Bull.*, 2015, **93**, 202–209.
37 M. R. Twiss, Standardized methods are required to assess and manage microplastic contamination of the Great Lakes system, *J. Great Lakes Res.*, 2016, **42**, 921–925.
38 A. McCormick, T. J. Hoellein, S. A. Mason, J. Schluep and J. J. Kelly, Microplastic is an Abundant and Distinct Microbial Habitat in an Urban River, *Environ. Sci. Technol.*, 2014, **48**, 11863–11871.
39 A. Collignon, J. H. Hecq, F. Galgani, F. Collard and A. Goffart, Annual variation in neustonic micro- and meso-plastic particles and zooplankton in the Bay of Calvi (Mediterranean-Corsica), *Mar. Pollut. Bull.*, 2014, **79**, 293–298.
40 A. Vianello, A. Boldrin, P. Guerriero, V. Moschino, R. Rella, A. Sturaro and L. Da Ros, Microplastic particles in sediments

of Lagoon of Venice, Italy: First observations on occurrence, spatial patterns and identification, *Estuarine, Coastal Shelf Sci.*, 2013, **130**, 54–61.

41 M. Claessens, S. De Meester, L. Van Landuyt, K. De Clerck and C. R. Janssen, Occurrence and distribution of microplastics in marine sediments along the Belgian coast, *Mar. Pollut. Bull.*, 2011, **62**, 2199–2204.

42 H. A. Leslie, S. H. Brandsma, M. J. M. van Velzen and A. D. Vethaak, Microplastics en route: Field measurements in the Dutch river delta and Amsterdam canals, wastewater treatment plants, North Sea sediments and biota, *Environ. Int.*, 2017, **101**, 133–142.

43 H. Bouwmeester, P. C. H. Hollman and R. J. B. Peters, Potential Health Impact of Environmentally Released Micro- and Nanoplastics in the Human Food Production Chain: Experiences from Nanotoxicology, *Environ. Sci. Technol.*, 2015, **49**, 8932–8947.

44 A. A. Koelmans, N. J. Diepens, I. Velzeboer, E. Besseling, J. T. K. Quik and D. van de Meent, Guidance for the prognostic risk assessment of nanomaterials in aquatic ecosystems, *Sci. Total Environ.*, 2015, **535**, 141–149.

45 P. E. Redondo-Hasselerharm, D. Falahudin, E. T. H. M. Peeters and A. A. Koelmans, Microplastic Effect Thresholds for Freshwater Benthic Macroinvertebrates, *Environ. Sci. Technol.*, 2018, **52**, 2278–2286.

46 A. A. Koelmans, E. Besseling, E. Foekema, M. Kooi, S. Mintenig, B. C. Ossendorp, P. E. Redondo-Hasselerharm, A. Verschoor, A. P. van Wezel and M. Scheffer, Risks of Plastic Debris: Unravelling Fact, Opinion, Perception, and Belief, *Environ. Sci. Technol.*, 2017, **51**, 11513–11519.

47 J. Gigault, H. El Hadri, S. Reynaud, E. Deniau and B. Grassl, Asymmetrical flow field flow fractionation methods to characterize submicron particles: application to carbon-based aggregates and nanoplastics, *Anal. Bioanal. Chem.*, 2017, **409**, 6761–6769.

48 L. J. Gimbert, K. N. Andrew, P. M. Haygarth and P. J. Worsfold, Environmental applications of flow field-flow fractionation (FIFFF), *TrAC, Trends Anal. Chem.*, 2003, **22**, 615–633.

49 F. A. Messaud, R. D. Sanderson, J. R. Runyon, T. Otte, H. Pasch and S. K. R. Williams, An overview on field-flow fractionation techniques and their applications in the separation and characterization of polymers, *Prog. Polym. Sci.*, 2009, **34**, 351–368.

50 A. Dehaut, A.-L. Cassone, L. Frère, L. Hermabessiere, C. Himber, E. Rinnert, G. Rivière, C. Lambert, P. Soudant, A. Huvet, G. Duflos and I. Paul-Pont, Microplastics in seafood: Benchmark protocol for their extraction and characterization, *Environ. Pollut.*, 2016, **215**, 223–233.

51 A. S. Tagg, M. Sapp, J. P. Harrison and J. J. Ojeda, Identification and Quantification of Microplastics in Wastewater Using Focal Plane Array-Based Reflectance Micro-FT-IR Imaging, *Anal. Chem.*, 2015, **87**, 6032–6040.

52 S. Primpke, C. Lorenz, R. Rascher-Friesenhausen and G. Gerdts, An automated approach for microplastics analysis using focal plane array (FPA) FTIR microscopy and image analysis, *Anal. Methods*, 2017, **9**, 1499–1511.

53 H. Dou, Y. J. Lee, E. C. Jung, B. C. Lee and S. Lee, Study on steric transition in asymmetrical flow field-flow fractionation and application to characterization of high-energy material, *J. Chromatogr. A*, 2013, **1304**, 211–219.

54 M. Cole, H. Webb, P. Lindeque, E. S. Fileman, C. Halsband and T. S. Galloway, Isolation of microplastics in biota-rich seawater samples and marine organisms, *Sci. Rep.*, 2014, **4**, 1–8.

55 W. Courtene-Jones, B. Quinn, F. Murphy, S. F. Gary and B. E. Narayanaswamy, Optimisation of enzymatic digestion and validation of specimen preservation methods for the analysis of ingested microplastics, *Anal. Methods*, 2017, **9**, 1437–1445.

56 M. G. J. Löder, H. K. Imhof, M. Ladehoff, L. A. Löschel, C. Lorenz, S. Mintenig, S. Piehl, S. Primpke, I. Schrank, C. Laforsch and G. Gerdts, Enzymatic purification of microplastics in environmental samples, *Environ. Sci. Technol.*, 2017, **51**, 14283–14292.

57 S. Kühn, B. van Werven, A. van Oyen, A. Meijboom, E. L. Bravo Rebolledo and J. A. van Franeker, The use of potassium hydroxide (KOH) solution as a suitable approach to isolate plastics ingested by marine organisms, *Mar. Pollut. Bull.*, 2017, **115**, 86–90.

58 E. Hermsen, R. Pompe, E. Besseling and A. A. Koelmans, Detection of low numbers of microplastics in North Sea fish using strict quality assurance criteria, *Mar. Pollut. Bull.*, 2017, **122**, 253–258.

59 C. Wesch, A. M. Elert, M. Wörner, U. Braun, R. Klein and M. Paulus, Assuring quality in microplastic monitoring: About the value of clean-air devices as essentials for verified data, *Sci. Rep.*, 2017, **7**, 5424.